Electron configuration and charge state of electrically active Cu, Ag and Au ions in ZnSe

2006 J. Phys.: Condens. Matter 18 8113

(http://iopscience.iop.org/0953-8984/18/34/020)

INSTITUTE OF PHYSICS PUBLISHING JOURNAL OF PHYSICS: CONDENSED MATTER

J. Phys.: Condens. Matter **18** (2006) 8113–8127 doi:10.1088/0953-8984/18/34/020

Electron configuration and charge state of electrically active Cu, Ag and Au ions in ZnSe

N D Nedeoglo[1,2,3,4], V P Sirkeli[1], D D Nedeoglo[1], R Laiho[2] and E Lähderanta[3]

[1] State University of Moldova, Mateevich street 60, MD-2009 Chişinău, Moldova
[2] Wihuri Physical Laboratory, University of Turku, FIN-20014 Turku, Finland
[3] Lappeenranta University of Technology, PO Box 20, FIN-53851 Lappeenranta, Finland

E-mail: nedeoglon@usm.md

Received 24 May 2006, in final form 18 July 2006
Published 14 August 2006
Online at stacks.iop.org/JPhysCM/18/8113

Abstract

The Hall effect, electrical conductivity and electron mobility are investigated at temperatures between 55 and 500 K in n-ZnSe crystals doped with Cu, Ag or Au. The presence of a small amount of Cu atoms leads to an inversion of the sign of the Hall coefficient at temperatures above 300 K. Anomalous temperature dependence of the electron mobility is observed in the samples with low Cu concentration (<0.3 at.% in the melt). Different characters of the temperature dependences of kinetic coefficients are found for n-ZnSe doped with Ag and Au. These curves are typical for crystals having several donor levels at different energetic depths. Immediately after doping, silver behaves like a usual compensating acceptor impurity while gold shows amphoteric properties. We propose a model that explains the anomalies of the temperature dependences of the kinetic coefficients in Cu-doped crystals and the lack of the anomalies in Ag-doped and Au-doped crystals. In accordance with this model and our experimental data, copper in n-ZnSe has two charge states, Cu^{+}_{Zn} (d^{10}) and Cu^{2+}_{Zn} (d^{9}), and two acceptor levels near the valence band. Silver and gold exist in single-charged states Ag^{+}_{Zn} and Au^{+}_{Zn} with d^{10} electron configuration forming single energy levels near the valence band. Au atoms form mainly interstitial Au_i donors at low doping concentrations and substitutional Au_{Zn} and Au_{Zn}-based acceptors at high doping concentrations. Time stimulation of the amphoteric properties of Ag is discussed.

1. Introduction

Transition metals such as Cu, Ag, and Au substitute isoelectronically for Zn atoms and form deep acceptor levels in the band gap of ZnSe single crystals. The occupation ordering of the d and s electron shells of these elements is modified so that they can be in two charge states,

[4] Author to whom any correspondence should be addressed.

0953-8984/06/348113+15$30.00

Cu^{+}_{Zn}, Ag^{+}_{Zn}, Au^{+}_{Zn} with d^{10} electron configuration [1–3] and Cu^{2+}_{Zn}, Ag^{2+}_{Zn}, Au^{2+}_{Zn} with d^{9} electron configuration [4–6]. Due to mixing of the d, p and s states, the acceptor levels formed in the band gap are electrically and optically active.

On the other hand, rapid cooling of the samples after annealing in dopant melts favours the formation of interstitial defects. As the number of the dopant elements is increased, the probability of the formation of interstitial donors such as Cu_i, Ag_i, and Au_i increases because of the increasing difference between the ionic radii of the dopant elements, 0.96 Å (Cu), 1.13 Å (Ag), 1.37 Å (Au) [7], and zinc, 0.83 Å [7]. Silver and gold atoms substituting zinc induce strains in the zinc sublattice since their size exceeds that of the zinc vacancy (V_{Zn}). As the interatomic Zn–Zn distance, 4.01 Å [8], is much larger than the ionic radius of the Ag and Au atoms, these dopants form mainly interstitial defects. The impurities, which can form both substitutional and interstitial defects and both acceptor and donor levels in the band gap, are called amphoteric impurities. Thus, the amphoteric properties of Cu, Ag, and Au impurities in ZnSe should become more evident with increasing element number, i.e., from copper to gold.

Currently, the question of the charge states and configuration of the electron shells of Cu_{Zn}, Ag_{Zn} and Au_{Zn} ions in ZnSe is open to discussion. The energetic positions of the sixfold degenerated T_2 levels calculated in [9] are $E_V + 0.46$ eV for Ag_{Zn}, $E_V + 0.63$ eV for Au_{Zn}, slightly deeper in comparison with $E_V + 0.26$ eV for Cu_{Zn}. The copper impurity is known to be more prone to formation of an unoccupied d^9-shell than the silver and gold impurities [2]. This was explained by the smaller atomic number of Cu within the limits of the same isoelectronic line and the smaller electronegativity associated with Ag and Au. It was also suggested [2] that Ag^{+}_{Zn} and Au^{+}_{Zn} ions have the usual d^{10} configuration and the formation of Ag^{2+}_{Zn} and Au^{2+}_{Zn} ions with d^9 configuration is impossible. According to optically detected magnetic resonance (ODMR) investigations [5, 6], silver and gold ions have the d^9 electron configuration.

In this paper, we discuss the charge states, the electron configuration and the amphoteric properties of copper, silver and gold impurities in n-ZnSe single crystals. The results are based on the measurements of the temperature dependences of the electrical conductivity, the Hall effect and mobility of charge carriers.

2. Experimental methods

The samples were doped with Cu, Ag or Au by long-term (100 h) high-temperature ($T_{\text{annealing}} = 950\,^{\circ}\text{C}$) annealing of high-resistive ($\rho = 10^8$–10^9 Ω cm) n-ZnSe single crystals in Zn + Cu, Zn + Ag or Zn + Au melts. The doping level was varied by changing the Cu content in the Zn melt from 0.05 to 0.75 at.%, the Ag content from 0.1 to 15 at.% or the Au content from 0.05 to 10 at.%. Metallic zinc double purified by vacuum sublimation and Cu, Ag and Au of 99.9999% purity were used for annealing the samples in quartz ampoules evacuated down to $p = 10^{-4}$ Torr and placed in a vertical furnace. After annealing, the ampoules were rapidly cooled down to room temperature. The surfaces of the samples were etched in 7% Br–CH_3(OH) solution and boiled in 40% NaOH. Rectangular bars of size $1 \times 1.5 \times 5$ mm^3 were used for measurements of the Hall effect, electrical conductivity and mobility of charge carriers at temperatures between 55 and 550 K and magnetic field of 1 T. The indium ohmic contacts were fabricated by the dot alloying method in vacuum for 20 min at 350 °C. The ohmicity of the contacts was controlled by the linearity of current–voltage curves.

3. Experimental results

3.1. n-ZnSe:Zn:Cu crystals

The temperature dependences of the Hall coefficient, R_H, for ZnSe:Cu crystals with different amounts of Cu are shown in figure 1. Series A (figure 1(a)) and series B (figure 1(b)) differ

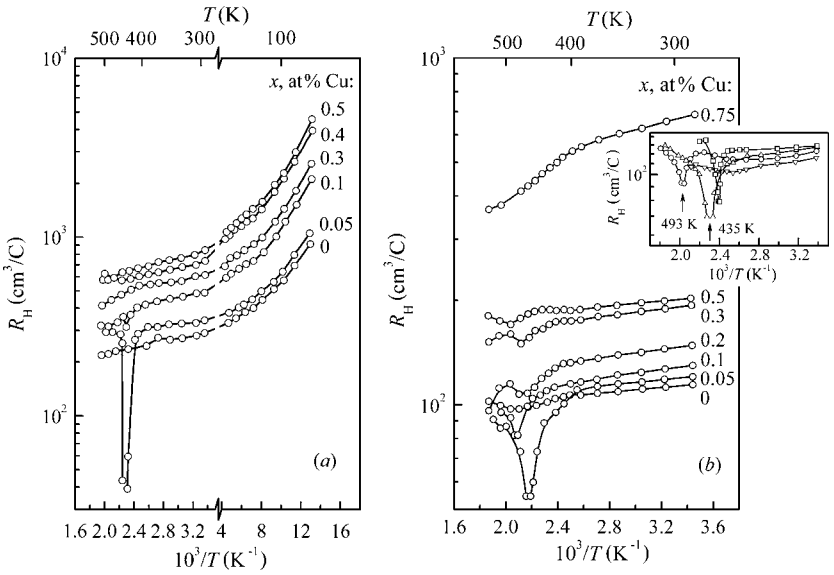

Figure 1. Temperature dependence of the Hall coefficient for n-ZnSe samples annealed in Zn + x at.% Cu melt (series A (a) and B (b)). Inset: temperature dependence of the Hall coefficient for n-ZnSe sample, annealed in Zn + 0.05 at.% Cu melt, after heat treatment in vacuum at $T = 413$ K for 0 (△), 5 (○), 10 (▽) h and after keeping at normal room temperature in air and darkness for eight months (□).

in the concentration of V_{Zn} native defects in the original crystals. The doping conditions for both series of samples were identical. Between temperatures of 77 and 300 K, the shape of the $R_H(10^3/T)$ curves does not depend on the Cu content in the Zn melt. R_H is found to decrease with increasing temperature (figure 1(a)) due to activation of electrons to the conduction band from shallow donors formed by a non-controllable impurity. The $R_H(10^3/T)$ dependence becomes weaker and tends to saturation near 300 K. However, upon further increase of T, the Hall coefficient decreases towards a new saturation due to ionization of a deeper donor level and its exhaustion.

For $T > 380$ K, R_H decreases slightly and monotonically with increasing temperature of the sample annealed in pure Zn melt. The addition of 0.05 at.% Cu into the melt results in an inversion of the sign of the Hall coefficient. Increase of the Cu content shifts the temperature of the sign inversion of R_H slightly towards higher temperatures and then leads to a gradual decrease of this anomaly (figure 1(b)). It is also found that the anomaly of R_H disappears during long-term high-temperature treatment of the doped samples in vacuum. The temperature dependences of R_H in the sample annealed in Zn + 0.05 at.% Cu melt are shown in the inset of figure 1(b) for various durations of the sample treatment at 413 K. During the first five hours, heating shifts the temperature of the R_H sign inversion from 435 to 493 K. Further heating for subsequent five hours quenches this anomaly, but it can be returned by keeping the samples for eight months at normal room conditions in darkness. After repeated heat treatment in vacuum for 25 h, the anomaly disappears completely.

The temperature dependences of the electrical conductivity, σ, of n-ZnSe samples with various Cu concentrations are shown in figure 2. As T decreases, the conductivity of the original sample increases, reaching a maximum at 100 K, and then decreases. The high-temperature branch of this maximum is caused by increasing electron mobility when the

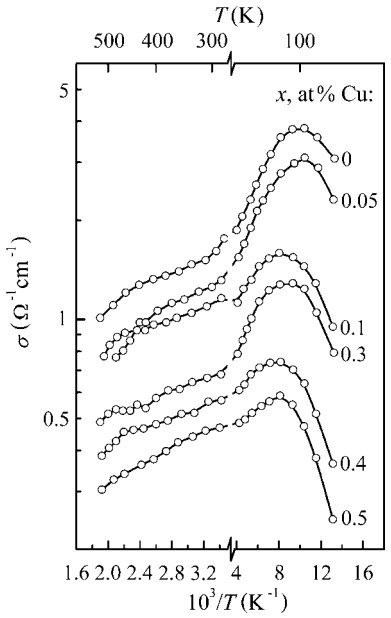

Figure 2. Temperature dependence of the electrical conductivity of n-ZnSe samples annealed in Zn + x at.% Cu melt (series A).

free electron concentration decreases with decreasing T. The low-temperature branch of this maximum is determined by a more intensive decrease of the free electron concentration and a greater contribution of scattering by impurity ions. Introducing Cu, which is a compensating impurity, into n-ZnSe reduces the values of σ in the whole temperature range and slightly changes the shape of the $\sigma(10^3/T)$ curve. With increasing Cu concentration, the maximum of this curve shifts towards higher temperatures due to increasing impurity scattering. No anomaly is observed in the $\sigma(10^3/T)$ dependence.

The temperature dependence of the electron Hall mobility, $\mu = R_H\sigma$, has an anomalous shape above 300 K in the 'anomalous' crystals (figure 3). Starting at 400 K, the mobility decreases quickly down to very low values and then sharply increases to the previous level. As the Cu concentration is increased, the anomaly of $\mu(T)$ becomes less marked.

3.2. n-ZnSe:Zn:Ag crystals

Figure 4 shows the temperature dependences of R_H measured immediately after doping the samples with Ag. The curves are typical for semiconductors having several local donor levels, i.e. there are two exponential parts, each followed by saturation. With temperature rise, R_H decreases due to electron activation from the shallowest donor level and the curves tend to saturation at $T > 100$ K due to exhaustion of the donor level. The increase of T above 300 K leads again to an exponential decrease of R_H with a far larger slope due to the activation of electrons from the second deeper donor level. This donor level is exhausted at $T > 400$ K. The slopes of the exponential part of the curves give the energies of the corresponding donor levels. Increase of the Ag content in the samples increases R_H, manifesting the compensating effect of the Ag impurity. A shift of the onset of the electron activation from the deeper donor level towards lower temperatures is observed as the Ag content is increased. This is stipulated by the fact that when the compensation of the shallow donors increases and their contribution

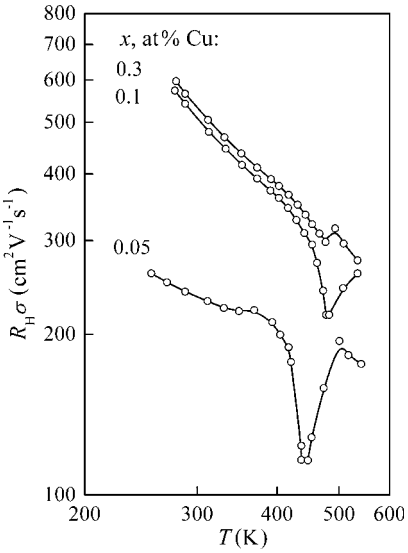

Figure 3. Temperature dependence of the electron Hall mobility in n-ZnSe samples annealed in Zn + x at.% Cu melt (series B).

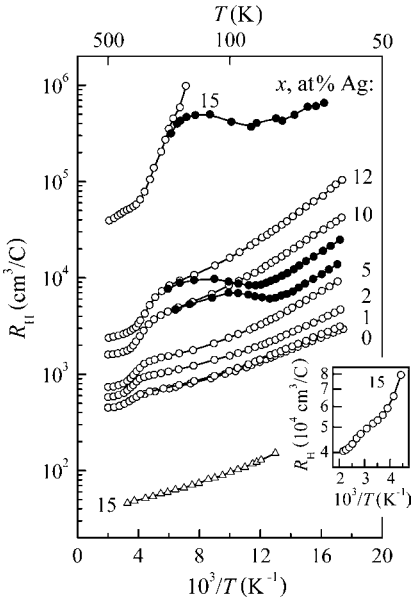

Figure 4. Temperature dependence of the Hall coefficient for n-ZnSe samples annealed in Zn + x at.% Ag melt ((○) in the dark, (●) under illumination, and (Δ) after storage for five years under normal room conditions). Inset: the high-temperature range of the $R_H(10^3/T)$ dependence in semi-logarithmic scale for the sample annealed in Zn + 15 at.% Ag melt.

to the total concentration of the charge carriers in the conduction band decreases, the activation process from the deeper donor level manifests itself more distinctly.

The deeper donor level is most clearly revealed at the maximum Ag content in the Zn melt (15 at.% Ag). The resistivity of this sample increases sharply with decreasing temperature due

Table 1. Electrical parameters of n-ZnSe:Zn:Ag crystals.

	$T = 300$ K			$T = 77$ K				
x (at.% Ag)	n (10^{16} cm^{-3})	σ (Ω^{-1} cm^{-1})	$R_H\sigma$ (cm^2 V^{-1} s^{-1})	n (10^{15} cm^{-3})	σ (Ω^{-1} cm^{-1})	$R_H\sigma$ (cm^2 V^{-1} s^{-1})		
1	1.20	0.89	467	4.0	1.99	3100		
2	0.88	0.68	481	2.8	1.33	2900		
5	0.73	0.53	456	1.6	0.59	2290		
10	0.36	0.25	441	0.42	0.11	1670		
12	0.23	0.15	413	0.21	0.003	959		
15	0.016	0.007	368	—	4.4×10^{-6}	—		
	After storage at normal room temperature for 5 years							
15	13.43	7.80	364	42.43	4.67	690		
x (at.% Ag)	N_D (10^{16} cm^{-3})	N_A (10^{16} cm^{-3})	$K = \frac{N_A}{N_D}$	E_D (meV)	n_0 (10^{15} cm^{-3})	N_D^{deep} (10^{15} cm^{-3})	E_D^{deep} (meV)	
1	6.0	4.9	0.82	9.2	10.6	4.5	130	
2	4.8	4.0	0.84	10.6	7.6	4.0	130	
5	4.1	3.6	0.88	13.1	5.2	3.6	130	
10	3.6	3.4	0.95	15.4	1.6	2.6	130	
12	2.7	2.6	0.97	18.2	0.88	1.9	130	
15	—	—	—	—	—	—	140	
	After storage at normal room temperature for 5 years							
	—	—	—	—	—	—	—	

to the very high compensation of the shallow donors. Measurements of the Hall coefficient at low temperatures are thus hampered, and we cannot observe the electron activation from shallow donors. However, the exponential decrease of R_H is observed again after exhaustion of the deeper donor level (figure 4, inset) indicating an activation process from the third, deepest donor level. A tendency to exhaustion of this level is observed at $T \approx 500$ K.

For a semiconductor partially compensated by acceptors with concentration N_A and having only one type of donor with concentration N_D, the temperature dependence of the electron concentration n in the conduction band can be expressed as

$$\frac{n\,(N_A + n)}{N_D - N_A - n} = \frac{N_C}{g} \exp\left\{-\frac{E_D}{k_B T}\right\}, \tag{1}$$

where g is the degeneracy of the donor state (for ZnSe $g = 2$), E_D is the activation energy of the donor impurity and N_C is the density of states in the conduction band. The values of N_D, N_A and E_D calculated by least-square fitting of the experimental data to (1) are given in table 1.

For a semiconductor also having deeper impurity levels with concentration N_{deep} and ionization energy E_{deep}, the temperature dependence of the free electron concentration is given by the equation

$$\frac{n\,(n - n_0)}{N_{deep} + n_0 - n} = \frac{N_C}{g_1} \exp\left\{-\frac{E_{deep}}{k_B T}\right\}, \tag{2}$$

where g_1 is the degeneracy of the deeper level and n_0 is the concentration of the electrons activated from shallow donors in the region of their exhaustion. The calculated values of N_{deep} and E_{deep} are given in table 1. For the sample with the highest content of the compensating impurity (15 at.% Ag in the melt), the activation energy of the electrons from the deeper level was also found from the slope of $\lg R_H T^{3/4}$ versus $10^3/T$ plot, equal to 140 meV. This value is

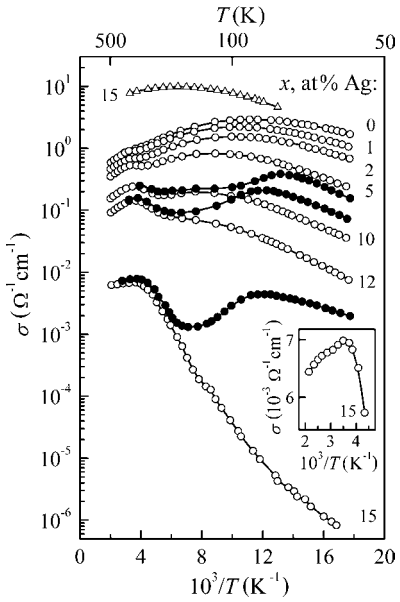

Figure 5. Temperature dependence of the electrical conductivity of n-ZnSe samples annealed in Zn + x at.% Ag melt ((○) in the dark, (●) under illumination, and (Δ) after storage for five years under normal room conditions). Inset: the high-temperature range of the $\sigma(10^3/T)$ dependence in semi-logarithmic scale for the sample annealed in Zn + 15 at.% Ag melt.

in good agreement with the one calculated using (2) within the limits of experimental accuracy. Table 1 shows that increasing Ag concentration results in the increase of both the compensation ratio $K = N_A/N_D$ and the activation energy of shallow donor impurities. As a result of the lack of compensation of the deeper donor level, the activation energy of electrons from this level, 130 meV, remains constant.

The temperature dependences of the electrical conductivity of the n-ZnSe single crystals doped with Ag are shown in figure 5. A high-temperature maximum appears and its magnitude increases with increasing Ag concentration in the Zn melt. The high-temperature branch of this maximum is determined by the temperature dependence of μ in the region of scattering by phonons where the concentration of the electrons is practically unchanged. With further decrease of the temperature, the conductivity decreases due to transitions of the electrons from the conduction band to the deeper donor level. Figure 5 shows that the onset temperature of this process is shifted towards lower temperatures with increasing Ag concentration. Our Hall measurements confirm this fact. The high-temperature branch of the low-temperature maximum in the $\sigma(10^3/T)$ dependence is determined by the charge carrier mobility that increases with decreasing temperature. In this case, the electron concentration depends weakly on the temperature since the shallow donor level is practically exhausted and the activation from the deeper level is quite low. The position of this maximum is determined by the maximum of $\mu(T)$ (figure 6) that shifts towards higher temperatures with increasing Ag content in the samples. Its relative value decreases because of the increasing role of electron scattering by impurity ions. The low-temperature branch of this maximum is determined by transitions of the electrons from the conduction band to shallow donors.

In the most compensated sample (15 at.% Ag in the melt), the low-temperature maximum in the $\sigma(10^3/T)$ dependence disappears since the activation of the electrons from the shallow

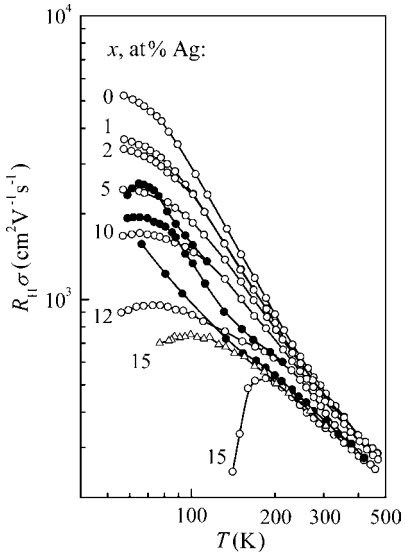

Figure 6. Temperature dependence of the electron Hall mobility in n-ZnSe samples annealed in Zn + x at.% Ag melt ((○) in the dark, (●) under illumination, and (Δ) after storage for five years under normal room conditions).

donor level is nearly absent. Transitions of the electrons from the conduction band to the deeper donor level cause a sharp decrease of σ. Slowing down of this process at low temperatures causes some flattening of this dependence near liquid nitrogen temperature. The conductivity of this sample is nearly unchanged at high temperatures above 250 K. However, a more accurate analysis (figure 5, inset) reveals a non-monotonic increase of σ with temperature decrease. This high-temperature peculiarity is caused by the competing contributions of mobility and concentration of electrons activated from the third deepest donor level. Without this level, σ would have increased monotonically with decreasing temperature (the mobility increases, but the concentration of the electrons activated from the second donor level is constant). Hall measurements confirm this model, too.

Investigations made immediately after doping the samples with Ag show that silver is a compensating acceptor in ZnSe. It is found that five-year storage of Ag-doped samples at room temperature in darkness in air dramatically increases the electrical conductivity and the concentration of free electrons and shallow donors. This can be observed, for instance, from the curves in figures 4 and 5 for the sample annealed in Zn+15 at.% Ag and measured immediately after doping with Ag and after storage of five years. The shape of the $\sigma(10^3/T)$ dependence indicates decreasing compensation of the donor impurity. These changes are most prominent in the samples with high Ag content, giving evidence of electrically active Ag-related shallow donors. Thus, silver shows amphoteric properties stimulated by room-temperature storage resulting in an increase of shallow Ag_i donors at the expense of Ag_{Zn} acceptors and, as a consequence, in the formation of the Ag-donor impurity band [10].

The temperature dependences of μ in the investigated samples are shown in figure 6. In the pure crystal, μ increases with decrease of T, which is characteristic of electron–phonon scattering. The flattening of the $\mu(T)$ dependence below 80 K is due to the contribution of scattering by impurity ions. As the Ag concentration is increased, the scattering by impurity ions is observed at higher temperatures: the slope of the high-temperature part of the curve decreases and a maximum appears. The relative height of the maximum decreases and it

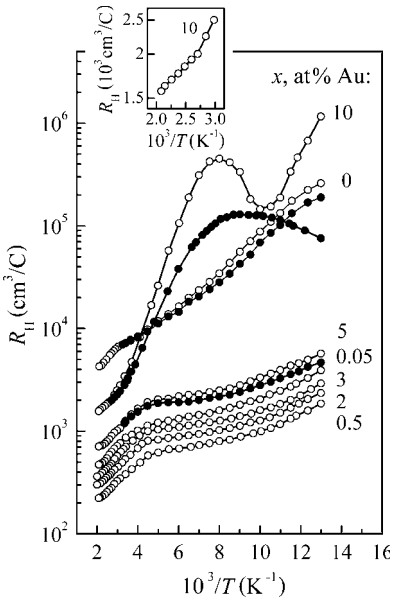

Figure 7. Temperature dependence of the Hall coefficient for n-ZnSe samples annealed in Zn+x at.% Au melt ((○) in the dark, and (●) under illumination). Inset: the high-temperature range of the $R_H(10^3/T)$ dependence in semi-logarithmic scale for the sample annealed in Zn + 10 at.% Au melt.

shifts towards higher temperatures as the Ag content is increased. Such evolution is stipulated by competition of electron scattering between impurity ions specific to low temperatures and phonons at high temperatures.

The scattering by impurity ions in the most heavily doped sample (15 at.% Ag) is observed up to the highest temperatures. Therefore, the slope of the $\mu(T)$ curve decreases in the region of phonon scattering. The very sharp decrease of μ below 200 K cannot be attributed to scattering by impurity ions, but rather to the appearance of collective potential barriers hampering the transport of carriers in strongly compensated semiconductors [11]. Illumination of the sample with white light sharply increases the concentration of conduction band electrons, which may shield random impurity potentials. As a result of reduced collective potential barriers, the anomaly disappears (see the curves with closed symbols in figure 6). This anomalous part also disappears after five-year storage of the samples at normal room temperature, which is an additional argument in favour of decreasing compensation of the donors due to transition of the silver impurity from acceptors (Ag_{Zn}) to donors (Ag_i) by displacing into interstitial sites [10].

3.3. n-ZnSe:Zn:Au crystals

The temperature dependences of R_H for Au-doped n-ZnSe crystals are shown in figure 7. The curves for undoped and moderately doped samples (<10 at.% Au in the Zn melt) are typical of the case of two electrically active donor levels. As the temperature increases, the Hall coefficient first decreases due to activation of electrons from a shallow donor level, tends to saturation and decreases again due to activation of electrons from a deep donor level. The electrical parameters calculated with (1) and (2) are shown in table 2. A strongly compensated ($K = 0.87$) non-controllable donor impurity in the original undoped crystal has an activation energy of ∼30 meV. Light doping with gold (0.5 at.% Au) reduces both the compensation of

Table 2. Electrical parameters of n-ZnSe:Zn:Au crystals.

	$T = 300$ K			$T = 77$ K			
x (at.% Ag)	n (10^{15} cm^{-3})	σ (Ω^{-1} cm^{-1})	$R_H\sigma$ (cm^2 V^{-1} s^{-1})	n (10^{15} cm^{-3})	σ (Ω^{-1} cm^{-1})	$R_H\sigma$ (cm^2 V^{-1} s^{-1})	
0	0.87	3.1×10^{-5}	0.22	0.02	4.6×10^{-6}	1.2	
0.05	7.23	5.5×10^{-3}	4.8	1.6	3.0×10^{-3}	11.6	
0.5	16.4	5.5×10^{-2}	21.1	3.4	2.1×10^{-2}	39.6	
2	11.7	3.5×10^{-1}	186	2.7	4.2×10^{-1}	984	
3	9.4	5.7×10^{-1}	382	2.1	8.2×10^{-1}	2391	
5	5.2	4.0×10^{-2}	48.7	1.1	7.6×10^{-3}	43.3	
10	1.8	2.8×10^{-3}	9.6	0.0054	8.3×10^{-6}	9.6	

x (at.% Ag)	N_D (10^{16} cm^{-3})	N_A (10^{16} cm^{-3})	$K = \frac{N_A}{N_D}$	E_D (meV)	n_0 (10^{15} cm^{-3})	N_D^{deep} (10^{15} cm^{-3})	E_D^{deep} (meV)
0	0.72	0.63	0.87	29.7	0.94	0.058	106
0.05	2.5	1.9	0.77	21.0	5.7	1.1	164
0.5	3.2	2.2	0.68	22.5	10.4	2.0	176
2	2.7	1.9	0.71	24.0	7.9	1.5	178
3	2.5	1.8	0.73	21.5	6.5	1.4	180
5	1.6	1.2	0.78	20.5	3.4	6.5	180
10	—	—	—	—	—	32.0	189

the donor impurity ($K = 0.68$) and the activation energy ($E_D = 22.5$ meV). We attribute the main electrically active impurities in lightly Au-doped samples to interstitial Au_i atoms [12] with activation energy $E_D(Au_i) = (22 \pm 2)$ meV (table 2).

As the Au concentration in the Zn melt is increased to 5 at.%, the compensation of the donor impurity increases to $K = 0.78$, indicating that Au atoms go preferentially into vacancies of the Zn sublattice where they form Au_{Zn} acceptors compensating shallow donor impurities. We note that while the compensation of the donors increases, the concentration of electrically active donors and acceptors decreases. This can be explained by the formation of electrically inactive radiative recombination centres (Au_{Zn}–Au_i), if we suppose that the Au_i ions are donors and the Au_{Zn} ions are acceptors. These associative centres were found by investigation of edge photoluminescence spectra of ZnSe:Zn:Au crystals [12].

At high Au concentration in the melt (10 at.% Au), the shallow donor impurities are almost completely compensated and therefore the electrical properties of the sample are influenced by deep donors with activation energy $E_D^{deep} \approx 190$ meV. Reducing the temperature to 125 K results in a rapid increase of R_H (figure 7). It is likely that this anomalous part of the $R_H(10^3/T)$ dependence observed below 125 K is associated with electron gas heating in electric field. A similar phenomenon has been observed in n-GaAs and n-InP crystals [13]. As R_H increases to $\sim 4 \times 10^5$ cm^3 C^{-1} with decreasing temperature, the resistivity of the sample rises and the electric field intensity increases up to ~ 30 V cm^{-1}. In such a strong field, the electrons have sufficient energy for ionization of impurity atoms by collision and therefore the free electron concentration increases and R_H decreases when T decreases from 125 to 100 K. This leads to decreasing resistivity of the sample and decreasing electric field intensity. This weakens the ionization by collisions and the free electron concentration again decreases due to freezing of the free electrons created by ionization. Under illumination of the samples with white light, R_H is diminished by four times (figure 7, $T \approx 125$ K) and the resistivity of the sample is considerably decreased (figure 8). As the electric field intensity decreases, ionization by

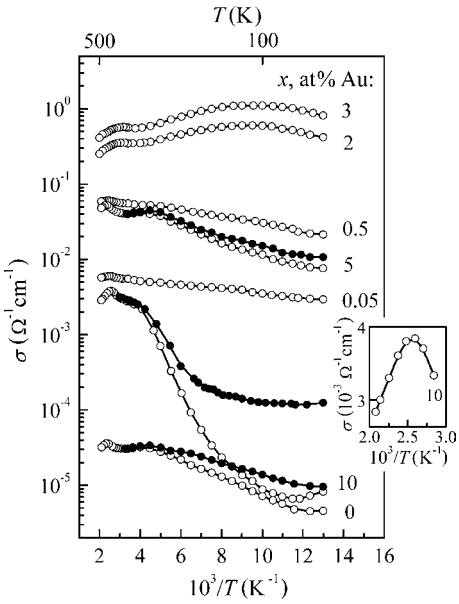

Figure 8. Temperature dependence of the electrical conductivity of n-ZnSe samples annealed in Zn+x at.% Au melt ((○) in the dark, and (●) under illumination). Inset: the high-temperature range of the $\sigma(10^3/T)$ dependence in semi-logarithmic scale for the sample annealed in Zn + 10 at.% Au melt.

collisions becomes almost impossible and the anomalous part of the $R_H(10^3/T)$ dependence disappears.

Figure 8 shows the shape of $\sigma(10^3/T)$ curve for Au-doped n-ZnSe. Two maxima are observed in the samples with low compensation of the donor impurities (2 and 3 at.% Au). As stated above, a similar shape of this curve is found for the Ag-doped n-ZnSe samples. The high-temperature maximum is due to the electrical activity of the deep donor level and the low-temperature one is caused by the shallow donor level associated with Au in the crystals. The contribution of the shallow donors to σ decreases with the increase of the Au concentration and the low-temperature maximum shifts towards higher temperatures and gradually disappears (5 and 10 at.% Au). Sensitivity of σ to illumination is observed for the samples with high Au concentration (5 and 10 at.% Au). Increase of the Au concentration increases σ in non-equilibrium state. However, in contrast to Ag-doped ZnSe, the shape of the $\sigma(10^3/T)$ dependence is unchanged, indicating small values of random impurity potential and drift and recombination barriers in the material [14]. A reason for this can be the moderate compensation ($K < 0.9$) of the donor impurity. Lack of sufficient random impurity potential in the sample with maximum Au concentration is an additional argument in favour of the above interpretation of the anomalous part in the $R_H(10^3/T)$ dependence for this sample.

The temperature dependences of μ in Au-doped n-ZnSe crystals are shown in figure 9. In the undoped sample, μ is very low due to high compensation and is weakly influenced by light. As the concentration of Au in the samples increases, the electron mobility increases considerably in the investigated temperature range (figure 9 and table 2, 0.05–3 at.% Au). The shape of the $\mu(T)$ curves indicates increasing contribution of scattering by phonons. For higher Au concentrations (5 and 10 at.% Au), the shape of these curves is complicated. The small maximum associated with the electrical activity of the deep donor level appears between $T = 400$ and 420 K. Sensitivity to the light is found at low temperatures.

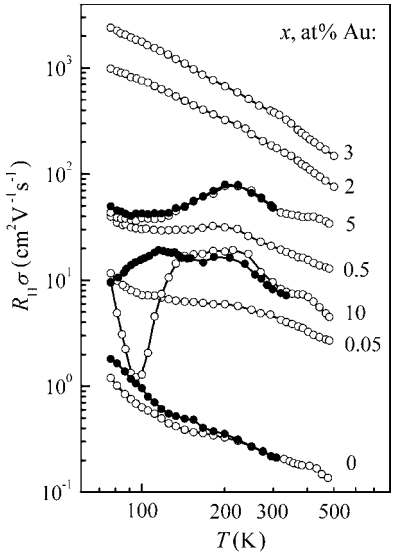

Figure 9. Temperature dependence of the electron Hall mobility for n-ZnSe samples annealed in Zn + x at.% Au melt ((○) in the dark, and (●) under illumination).

4. Discussion

Analysis of our experimental data shows that the anomalous temperature dependence of R_H caused by the sign inversion is observed only for lightly Cu-doped ZnSe crystals. In all the known cases when either double inversion of the sign of R_H in a p-type semiconductor or inversion of the sign in an n-type semiconductor is observed, the anomaly of $R_H(10^3/T)$ curve is associated with mixed electron–hole conductivity [15–18]. As a rule, this phenomenon has been observed in narrow band-gap semiconductors. Therefore, the models proposed with account of the specificity of these semiconductors are not valid for ZnSe, which has a wide energy gap ($E_g = 2.8$ eV at 77 K).

We explain the anomalies observed in the kinetic coefficients by the nature of the energy levels of transition metal ions in n-ZnSe. There are two acceptor-type energy levels that correspond to the charge states Cu^{+}_{Zn} (d^{10}) and Cu^{2+}_{Zn} (d^{9}) of copper. The more shallow Cu^{2+}_{Zn} acceptors have greater electron capture cross-section than the Cu^{+}_{Zn} acceptors, and, as well as the native V_{Zn} defects, they can compensate the shallow non-controlled donor impurity [1]. The energy level of the Cu^{2+}_{Zn} centre at 0.35 eV above the valence band [1] is thus completely occupied by electrons, while that of the Cu^{+}_{Zn} centre at 0.73 eV above the valence band [1] is unoccupied at low T. The thermal activation of the electrons from the valence band to this vacant level becomes effective at sufficiently high temperatures ($T > 400$ K, figure 1, 0.05 at.% Cu). The concentration of free holes in the valence band increases sharply, but the concentration of the conduction band electrons is constant due to exhaustion of the donor impurity. Thus, we observe electron–hole impurity conductivity that is the necessary condition for inversion of the sign of R_H in p- and n-type semiconductors [16, 18]. Theoretical calculations given in [18] for the temperature dependence of the Hall coefficient in two-layer structures show that in case of the carriers of opposite charges, the second inversion of the Hall coefficient is observed in addition to the classic inversion associated with the intrinsic conductivity of p-layer. These conclusions are valid for semiconductors with mixed electron–hole conductivity. If the hole

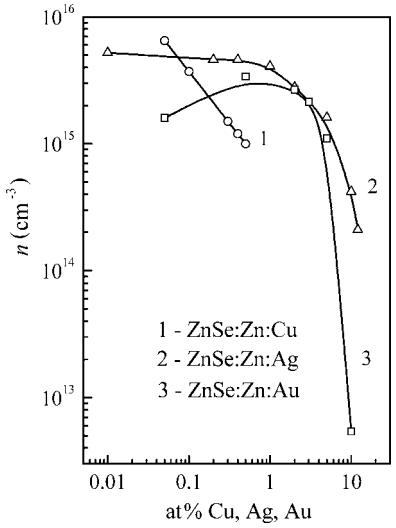

Figure 10. Influence of the concentration of Cu, Ag, and Au dopants on the free electron concentration in n-ZnSe crystals.

concentration decreases with temperature decrease and the electron concentration is unchanged, the second inversion of the Hall coefficient takes place.

The anomalous parts in the $R_H(10^3/T)$ and $\mu(T)$ dependences flatten and completely disappear with increasing Cu content. In accordance with the proposed model, we attribute this behaviour to redistribution of the Cu^+_{Zn} and Cu^{2+}_{Zn} concentrations which decreases the number of Cu^+_{Zn} centres responsible for the hole concentration in the valence band. Increase of the concentration of the Cu^{2+}_{Zn} acceptors with increasing Cu content in n-ZnSe crystals has been found from investigation of nonlinear absorption spectra [19] and luminescence spectra [20].

The gradual transition from the anomalous $R_H(10^3/T)$ dependence to the normal one during long-term high-temperature treatment of the samples in vacuum is caused, in our opinion, by motion of Cu atoms from Zn sublattice into interstitial sites which decreases the concentration of Cu^+_{Zn} and Cu^{2+}_{Zn}. Long-term storage of the samples at normal room temperature leads to diffusion of interstitial Cu_i atoms into the vacant sites of the Zn sublattice. As the concentration of these centres increases, the temperature dependence of R_H becomes anomalous. For Cu-doped n-ZnSe samples, the anomalies of $R_H(10^3/T)$ and $\mu(T)$ curves at high temperatures can therefore be explained by the existence of Cu atoms with d^{10} and d^9 electron configurations in the Zn sublattice.

The number of electrically active Cu_i defects in Cu-doped samples is insufficient for revealing the amphoteric properties of the dopant impurity. The gradually decreasing concentration of free electrons with increasing Cu content (figure 10) gives evidence for the acceptor nature of Cu in ZnSe. Interstitial Cu ions take part only in the formation of acceptor-type (Cu_{Zn}–Cu_i) and (Cu_{Zn}–V_{Se}–Cu_i) radiative recombination centres [21].

Within the limits of our model, the lack of anomalies of the kinetic coefficients in n-ZnSe doped with Ag and Au suggests that silver and gold in contrast to copper are simple single-charged Ag^+_{Zn} and Au^+_{Zn} acceptors with d^{10} electron configuration. These two impurities form near the valence band single levels, which can compensate the main electrically active impurities. The contribution of the shallow non-controlled donors to σ decreases with increasing Ag concentration. The deeper donor level with activation energy $\approx$130 meV

becomes a key centre that causes conductivity of the investigated crystals at high temperatures. The interstitial Au_i defects do not show electrical activity and free electron concentration decreases with increasing dopant content (figure 10). Thus, the measurements carried out immediately after doping the samples do not reveal amphoteric properties for Ag in ZnSe. However, the probability of the formation of donor-type Ag_i defects is higher in comparison with Cu_i. Our photoluminescence investigations confirm this statement, as the $I_2^{Ag_i}$-line attributed to radiative annihilation of the Ag_i-donor bound excitons is dominant in edge luminescence spectra of n-ZnSe:Zn:Ag crystals [22]. We have also found time stimulation of amphoteric properties of Ag in Ag-doped ZnSe [10].

At low Au contents in the Zn melt, the larger Au atoms (in comparison with Cu and Ag) are preferentially incorporated into interstitial sites and form a great number of electrically active Au_i donors. Thus, there is an effect of donor doping of n-ZnSe crystals with Au [23]. This process tends to saturation with increasing Au concentration and then simple Au_{Zn} acceptors and acceptor-type associative centres (Au_{Zn}–Au_i), (Au_{Zn}–V_{Se}) and/or (Au_{Zn}–D_{Zn}) are formed. At first a moderate and later a strong compensation of the donor impurities takes place, rapidly decreasing the free electron concentration (figure 10). The $I_2^{Ag_i}$-line attributed to radiative annihilation of the Au_i-donor bound excitons appears in the edge photoluminescence spectra of Au-doped ZnSe crystals. Its intensity first increases, as well as the concentration of free electrons, and then decreases with increasing Au content. The decreasing intensity of the $I_2^{Ag_i}$-line is accompanied by an emission band associated with Au_{Zn} acceptors and showing increasing intensity when the Au concentration is increased [23].

5. Conclusion

According to Hall measurements, the Au impurity has the most prominent amphoteric properties in n-ZnSe single crystals among Cu, Ag and Au impurities, as it forms a great number of Au_i donors, as well as Au_{Zn} acceptors, immediately after doping. Electrical measurements show that silver and gold ions introduced into vacant sites of the Zn sublattice form simple single-charged Ag_{Zn}^{+} and Au_{Zn}^{+} states with d^{10} electron configuration. Copper ions can form both single-charged Cu_{Zn}^{+} (d^{10}) and double-charged Cu_{Zn}^{2+} (d^{9}) centres giving rise to impurity electron–hole conductivity in Cu-doped ZnSe crystals.

Acknowledgments

We thank Dr V A Kasiyan (State University of Moldova) for doping the crystals with Cu and Ag and assistance in measurements. NDN thanks the Wihuri Physical Laboratory, University of Turku, for warm hospitality and the Lappeenranta University of Technology Foundation.

References

[1] Stringfellow G B and Bube R H 1968 *Phys. Rev.* **171** 903
[2] Dean P J, Fitzpatrick B J and Bhargava R N 1982 *Phys. Rev.* B **26** 2016
[3] Holtz P O, Monemar B and Łożykowski H J 1985 *Phys. Rev.* B **32** 986
[4] Godlewski M, Lamb W E and Cavanett B C 1981 *Solid State Commun.* **39** 595
[5] Poolton N R J, Davies J J, Nicholls J E and Fitzpatrick B J 1985 *J. Cryst. Growth* **72** 336
[6] Poolton N R J, Nicholls J E and Davies J J 1988 *J. Cryst. Growth* **86** 609
[7] Kittel Ch 1971 *Introduction to Solid State Physics* (New York: Wiley)
[8] Aven M and Prener J S (ed) 1967 *Physics and Chemistry of II–VI Compounds* (Amsterdam: North-Holland)
[9] Chacham H, Alves J L A and DeSiqueira M L 1986 *Solid State Commun.* **60** 411

[10] Laiho R, Lashkul A V, Lähderanta E, Nedeoglo D D, Nedeoglo N D and Shakhov M A 2006 *Semicond. Sci. Technol.* **21** 654
[11] Kasiyan V A, Nedeoglo D D and Timchenko I N 1995 *Phys. Status Solidi* b **190** 501
[12] Nedeoglo N D, Avdonin A N, Ivanova G N, Nedeoglo D D, Kolibaba G V and Sirkeli V P 2005 *J. Lumin.* **112** 62
[13] Emel'yanenko O V, Nasledov D N and Nedeoglo D D 1973 *Sov. Phys.—Solid State* **15** 1147
[14] Bolboshenko V Z, Djouadi D, Kasiyan V A and Nedeoglo D D 1992 *Phys. Status Solidi* a **113** 121
[15] Petrovskii V I, Solov'ev N P, Omel'yanovskii E M and Ivleva V S 1978 *Fiz. Tekh. Poluprovdn.* **12** 1904 (in Russian)
[16] Ivanov-Omskii V I, Berchenko N N and Elizarov A I 1987 *Phys. Status Solidi* a **103** 11
[17] Elizarov A I, Ivanov-Omskii V I, Korniyash A A and Petryakov V A 1984 *Sov. Phys.—Semicond.* **18** 125
[18] Kuchis E V 1990 *Galvanomagnitnye Effecty i Metody Ikh Issledovaniya* (*Galvanomagnetic Effects and Their Investigation Methods*) (Moscow: Izd. Radio i Svyaz') (in Russian)
[19] Baltrameyunas R, Baubinas R, Vaitkus Iu, Gavryushin V and Rachyukaitis G 1985 *Sov. Phys.—Solid State* **27** 227
[20] Ivanova G N, Kasiyan V A, Nedeoglo D D and Oprea S V 1998 *Semicond.* **32** 154
[21] Bolboshenko V Z, Ivanova G N, Kalmykova I, Kasiyan V A, Nedeoglo D D and Novikov B V 1990 *Fiz. Tekh. Poluprovdn.* **24** 1929 (in Russian)
[22] Ivanova G N, Kasiyan V A, Nedeoglo D D and Nedeoglo N D 1999 *J. Lumin.* **82** 277
[23] Avdonin A N, Ivanova G N, Nedeoglo D D, Nedeoglo N D and Sirkeli V P 2005 *Physica* B **365** 217